Building Engineering 2024, 2(2), 1567.
https://doi.org/10.59400/be.v2i2.1567

Article

Finite elemental assessment of torsional behavior of RC beams having different shear reinforcement

Warda Jannat Juhin, Raihan Uddin Ahmed, H. M. A. Mahzuz*, Md. Ariful Islam

Department of Civil and Environmental Engineering (CEE), Shahjalal University of Science and Technology (SUST), Sylhet 3114, Bangladesh
*** Corresponding author:** H. M. A. Mahzuz, mahzuz_211@yahoo.com

CITATION

Juhin WJ, Ahmed RU, Mahzuz HMA, Islam MA. Finite elemental assessment of torsional behavior of RC beams having different shear reinforcement. Building Engineering. 2024; 2(2): 1567.
https://doi.org/10.59400/be.v2i2.1567

ARTICLE INFO

Received: 26 July 2024
Accepted: 13 October 2024
Available online: 25 October 2024

Abstract: In this paper, the torsional behavior of 8 beams in 4 categories with 2 different ultimate concrete compressive strengths (22.92 MPa and 43.47 MPa) was evaluated, and the best alternative of shear reinforcement pattern compared to the conventional non-welded rectangular stirrup beam (NRSB) was determined. 4 types of beams were modeled using SolidWorks, namely—Non-welded Rectangular Stirrup Beam (NRSB), Welded Rectangular Stirrup Beam (WRSB), Normal Welded Warren Truss-shaped Beam (NWWTB), and Flipped Welded Warren Truss-shaped Beam (FWWTB). The dimension and weight of reinforcement were kept the same for all beams. After simulating using ANSYS, it was seen that WRSB specimens had the largest torsional moment capacity, while NWWTB in normal orientation showed marginal improvement compared to NRSB.

Keywords: torsional behavior; concrete compressive strength; shear reinforcement pattern; non-welded rectangular stirrup beam (NRSB); welded rectangular stirrup beam (WRSB); ANSYS simulation

1. Research context and objectives

Reinforced concrete beam—a major structural element—through its lifetime faces shear stress, flexural stress, torsion, etc. Along with research on the flexural and shear capacity of reinforced concrete beams, a lot of research is also seen to be conducted on the torsional behavior as well. For example, Panchacharam and Belarbi [1] performed analysis on the torsional behavior of reinforced concrete beams strengthened with FRP composites. Deifalla and Ghobarah [2] developed an analytical model for torsional strengthening of reinforced concrete beams. Mahzuz et al. [3] conducted a study on the strength enhancement of RCC beams for different types of shear reinforcement. Three types of specimens—non-welded rectangular stirrup beam (NRSB), welded rectangular stirrup beam (WRSB), and welded Warren Truss beam (WWTB)—were prepared. All the specimens had the same concrete dimension and similar reinforcement weight. The experiment results showed that the load-carrying capacity of the WWTB was 35.28% more than the NRSB. Which exceeded WRSB, which showed a 10.16% increase in load-carrying capacity compared to NRSB.

Enhancing the beam capacity by using alternative techniques in an ongoing process of research [4,5]. Demir et al. [6] conducted a nonlinear finite element study using ABAQUS, showing a 20.8% shear capacity increase in RC T-beams with Diagonal Shear Reinforcement (DSR). Saju and Usha [7] conducted a study on the flexural strength of RC beams. From the results, it is found that 20% increase in RC beams with truss reinforcement compared to beams with normal vertical stirrups. The beams with truss reinforcement also deflected less than a normal rectangular stirrup beam. Al-Nasra and Asha [8] studied shear reinforcement types in RC beams, finding swimmer bars reduced crack width and length more effectively than traditional stirrups, with similar results for bolted and welded bars. Khan et al. [9] experimentally investigated shear reinforcement in RC beams using 45° swimmer bars. Beams with 3-legged swimmer bars showed a 9.3% higher load capacity than traditional stirrups, using 30% less shear steel. Another study discloses that WRSB specimens exhibit the maximum torsional moment (including the angle of twist) values for both mix ratios, with a range of 4.4% to 10% when compared to NRSB. However, for the WWTB specimens, the values are nearly the same, ranging from 2.4% to 1% compared to NRSB [10].

Several studies in the field of numerical simulation of RCC beams using ANSYS have been found to evaluate the capacity and strength of the beam with or without conducting an experimental test with acceptable accuracy. A work extends ANSYS modeling from smeared to a discrete approach, identifying shear cracks and simulating load-deflection curves, matching experimental results [11]. Using ANSYS, discrete modeling identified shear cracks and simulated load-deflection curves, matching experimental results. Monitoring vibration behavior and adjusting FEM parameters helped establish damage distribution in beams, with scanning laser equipment confirming modal updating's effectiveness [12]. Shear reinforcement in beams prevents premature collapse under high shear stress. Ensuring shear capacity exceeds flexural capacity helps to achieve ductile design, with failure mechanisms varying by dimensions, geometry, loading, and material properties [13]. Reinforced concrete beams face bending, transverse shear, and sometimes torsional forces. Torsion, often concurrent with bending and shear, is classified as primary or secondary. Effective torsional resistance requires closely spaced stirrups and longitudinal bars, with longitudinal bars alone improving strength by only 15% [14]. In another study, reinforced concrete beam behavior was analyzed under different shear reinforcement patterns using ANSYS software. Six 3D beams were analyzed for ultimate capacity, crack formation, and load-deflection response. All reinforcement types were similarly effective under static loading [15].

Hasan et al. [16] used ANSYS to simulate reinforced concrete beams with four shear reinforcement patterns: NRSB, WRSB, NWTB, and WWTB, analyzing flexural and shear capacities for different concrete strengths. Compared to NRSB, WWTB showed the highest load enhancement, up to 33.74%. The simulation closely matched experimental results, differing by 0.5% to 3%. Dahmani et al. [17] developed a 3D finite element model of RCC beams using ANSYS with SOLID65 elements and smeared reinforcement, validating simulation results against hand calculations. The results obtained through simulation using ANSYS were seen to be accurate as per validation. They showed the viability of using ANSYS software for analysis of RCC beams. Few researchers conducted experimental and non-linear finite element analyses of six RC beams under four-point bending using ANSYS Mechanical APDL 12.0. They compared results with IS 456:2000 code provisions, finding the code's analytical ultimate moment capacity slightly lower than experimental and FEA results [18,19]. Kandekar and Talikoti [20] studied the torsional behavior of RC beams wrapped with aramid fiber. Experimental and ANSYS simulations showed close results for ultimate loads, first cracking loads, angle of twist, and twisted beam shape. Rathi et al. [21] compared the torsional behavior of RC beams wrapped with CFRP and GFRP fabric. CFRP-wrapped beams showed greater torsional strength, angle of twist, and ductility factor than GFRP-wrapped beams.

One study numerically evaluates shear performance in reinforced concrete beams with different shear reinforcement patterns. Continuous systems (SSSSRS and DSSSRS) show 14.4% and 19.8% improved shear performance over conventional stirrups [22]. On the other hand, the nonlinear behavior of RC beams even post-tension beams is complex due to various parameters. Analysis was done by four-point bending tests on RC beams using ANSYS, considering concrete properties, mesh density, steel cushions, shear reinforcement, and convergence criteria. The findings aim to enhance ANSYS analysis guidelines for RC beams [23,24]. Another study investigates the behavior of shallow reinforced concrete beams under transverse loading using finite element analysis with ANSYS software. It focuses on stress distribution, cracks, and load-deflection relationships. Concrete is modeled with Solid65 eight-noded elements and an elastoplastic work hardening model, terminating at crushing. Reinforcement is modeled with Link180 elements, with linear elastic behavior before yield and perfectly plastic beyond that [25]. Finite Element Analysis (FEA) simulations are highly versatile, allowing for the effective modeling and analysis of even non-homogeneous numerical problems. This capability enables FEA to achieve satisfactory accuracy when compared to lab-based experiments [26–29].

Despite extensive research on the torsional behavior and shear reinforcement of reinforced concrete (RC) beams, there remains a significant gap in comprehensive studies using advanced numerical simulations to analyze different shear reinforcement patterns under torsional loads. Though there are few studies as mentioned above, a detailed numerical investigation using ANSYS on the torsional behavior of RC beams with different shear reinforcement patterns has not been thoroughly explored. This study aims to fill this gap by conducting a nonlinear finite element analysis (FEA) using ANSYS to compare the torsional performance of RC beams with various shear reinforcement configurations. By doing so, it seeks to provide deeper insights into optimizing shear reinforcement for enhanced torsional resistance, potentially reducing the need for extensive experimental testing and offering more efficient design solutions for structural engineers.

Based on the above contextual foundation, the knowledge gap is clearly identified. Therefore, the objective of this research is:

- To analyze the torsional behavior of reinforced concrete beams with four different types of shear reinforcement patterns (NRSB, WRSB, NWWTB, FWWTB) using ANSYS.
- To identify the most effective shear reinforcement pattern in enhancing torsional resistance compared to the conventional non-welded rectangular stirrup beam (NRSB).

2. Research method

2.1. Selection of models

In total, eight beams were modeled, and their torsional behavior was analyzed. These eight beams were divided into three patterns with two different concrete compressive strengths. All the beams were of the same dimension, i.e., length = 1220 mm, width = 127 mm, and height = 203 mm. The concrete cover for reinforcement was 30.5 mm on the sides and 43.5 mm on the top and bottom faces, meeting the minimum requirements. The reinforcement patterns of NRSB, WRSB, NWWTB, and FWWTB are shown in **Figures 1–4**. All the flexural reinforcements were 16 mm dia rebar, and all the shear reinforcements were 100 mm dia bars. To observe the effect of torsion, the weight of steel in all patterns is kept the same. Thus, the costs of the different patterns of the beam were the same. This could make the comparison easier. The flow diagram of the study is shown in **Figure 5**.

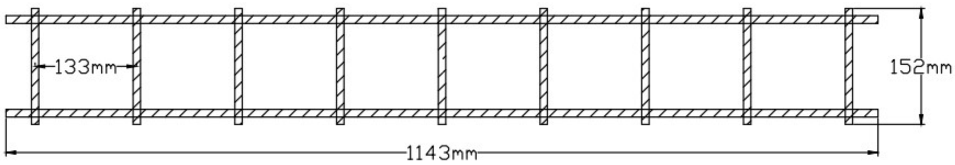

Figure 1. NRSB reinforcement pattern and dimension.

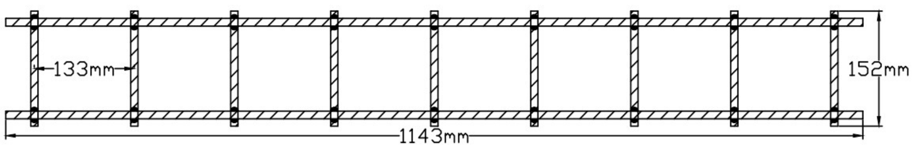

Figure 2. WRSB reinforcement pattern and dimension.

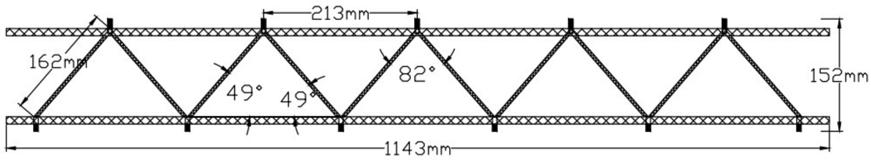

Figure 3. NWWTB reinforcement pattern and dimension.

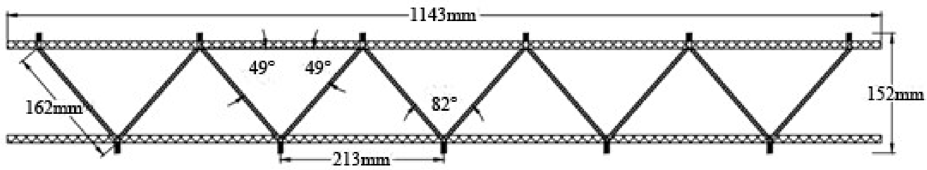

Figure 4. FWWTB reinforcement pattern and dimension.

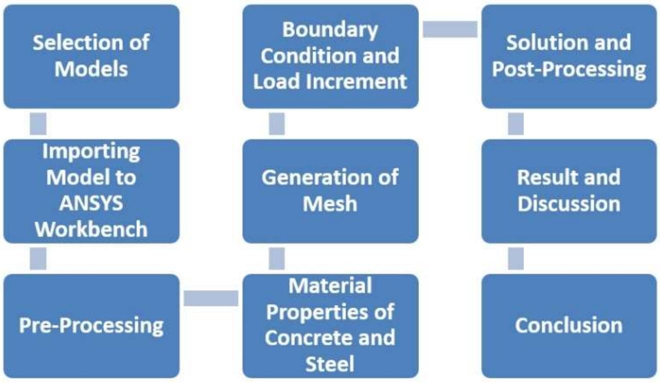

Figure 5. Flow diagram of research method.

The concrete model and the different reinforcement models are shown in **Figures 6–9**. Note that the truss models were created using SolidWorks and later exported to ANSYS Workbench.

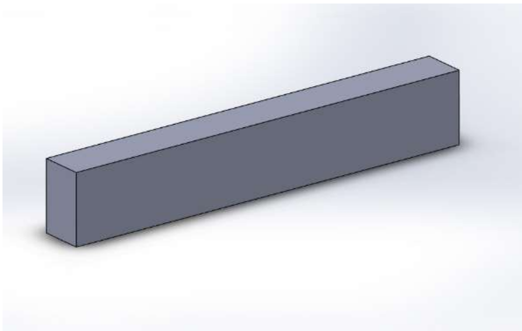

Figure 6. Created concrete model in solid works.

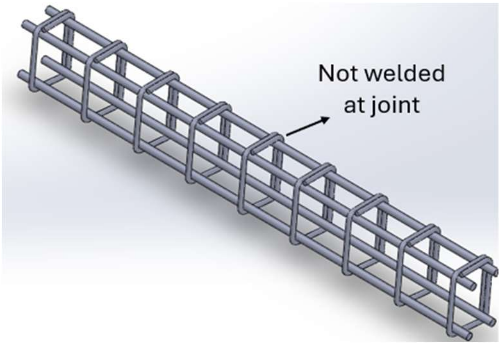

Figure 7. NRSB reinforcement model.

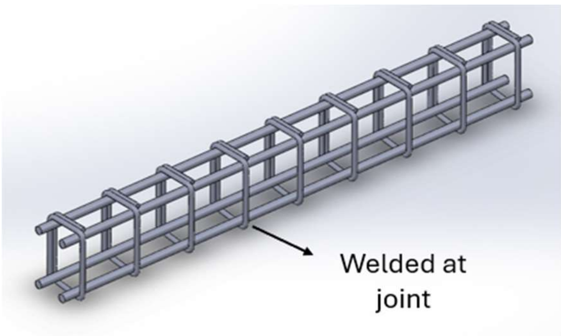

Figure 8. WRSB reinforcement model.

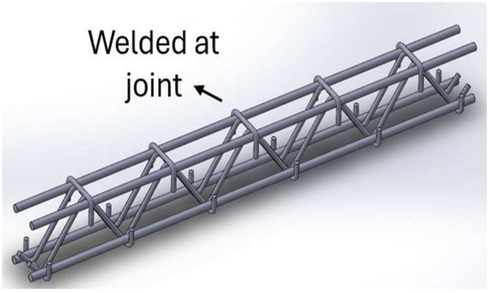

Figure 9. WWTB reinforcement model.

2.2. Importing model to ANSYS workbench

SolidWorks uses a proprietary file extension for image files called SLDPRT, which stands for SolidWorks Part file. ANSYS does not directly support the file format. So, in order to import the file to the ANSYS Workbench, the SLDPRT file needed to be transformed into a vendor-neutral file format that ANSYS supports, such as Parasolid, IGES, STEP, etc. The SLDPRT files were converted to IGES file format directly by using SolidWorks and then imported to ANSYS. The Initial Graphics Exchange Specification (IGES) is a vendor-neutral file format that allows the digital exchange of information among computer-aided design systems.

2.3. Pre-processing

The preprocessing process contains assigning the material properties of different parts, meshing, applying constraints, and applying loads. The preprocessing method will be discussed in brief within the next few chapters.

There are several methods to evaluate the non-linear behavior of concrete. In this paper, the modified Hognestad piecewise elastic model [30] was used to obtain the compressive uniaxial stress-strain relationship. The following Equations (1)–(4) were used to compute the engineering multilinear isotropic stress-strain curve for the concrete.

$$E_c = 4730\sqrt{f_c'} \tag{1}$$

$$f = \frac{E_c\,\varepsilon}{1+\left(\frac{\varepsilon}{\varepsilon_0}\right)^2} \tag{2}$$

$$\varepsilon_0 = \frac{2f_c'}{E_c} \tag{3}$$

$$E_c = \frac{f}{\varepsilon} \tag{4}$$

2.4. Material properties of concrete and steel

Elastic Perfectly Plastic Material Model was used for modeling the steel reinforcement materials. The grade of steel used in the beams was 500 W, i.e., the yield strength of steel is 500 MPa. The values of Young’s modulus, tangent modulus, and Poisson’s ratio were taken as 200,000 MPa, 1450 MPa, and 0.3, respectively. Two concrete compressive strengths are considered for the study; one is relatively low (22.92 MPa), and another is moderate (43.47 MPa) 28-day strengths. The stress-strain curve of steel and two different concrete compressive strengths are shown in **Figures**

10 and **11**. Mild steel electrodes were used, and the electrodes were E6012. The tensile strength of the electrode was 414 MPa. Bilinear isotropic hardening data were inserted, and material was assigned.

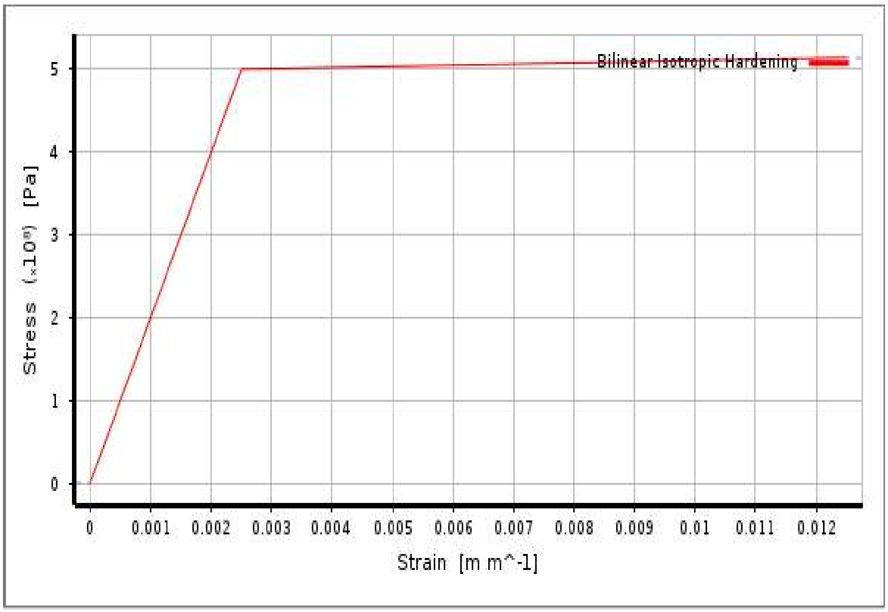

Figure 10. Stress-strain curve for steel reinforcement.

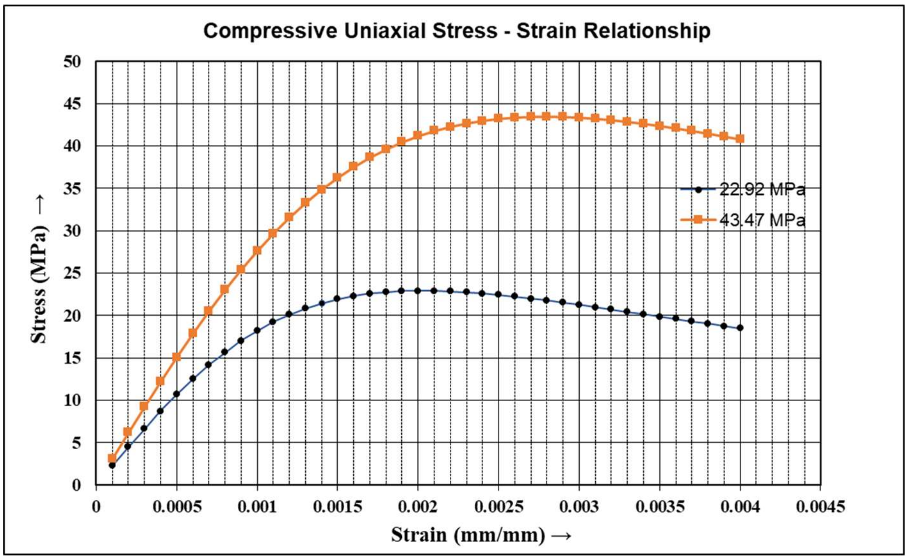

Figure 11. Uniaxial stress-strain curve for two different concrete compressive strengths (Poisson's ratio-0.18).

2.5. Generation of mesh

Meshing is an integral part of the computer-aided simulation process. The mesh affects the accuracy, convergence, and speed of the solution. Furthermore, the time it takes to create and mesh a model is often a significant part of the time it takes to get results from a CAE solution. The better and more automated the meshing tools, the better the solution. For solid models, ANSYS meshing technologies provide robust, well-shaped, quadratic tetrahedral meshing on even the most complex geometries. As the model is comprised of rectangular solids and cylindrical solids, the quadratic tetrahedral mesh was created in the patch confirming method. The mesh element size was 8 mm according to mesh sensitivity analysis. The number of elements varied from 66,411 to 66,832, and the number of nodes varied from 32,565 to 32,590 depending on the model. The meshed parts are shown in the following figures (**Figures 12–16**).

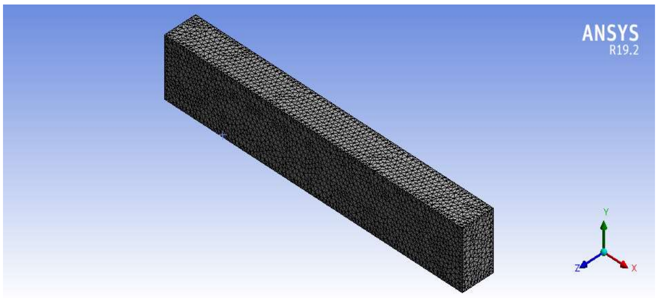

Figure 12. Concrete model after meshing.

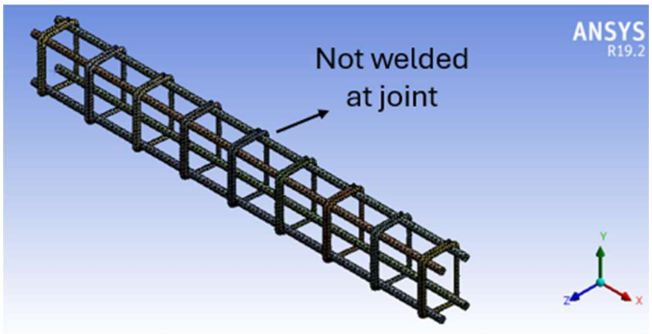

Figure 13. Meshed model of NRSB reinforcement.

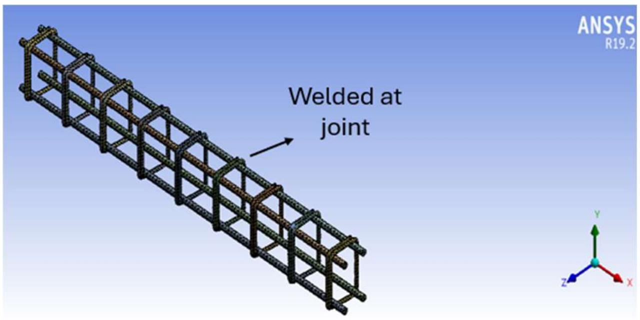

Figure 14. Meshed model of WRSB reinforcement.

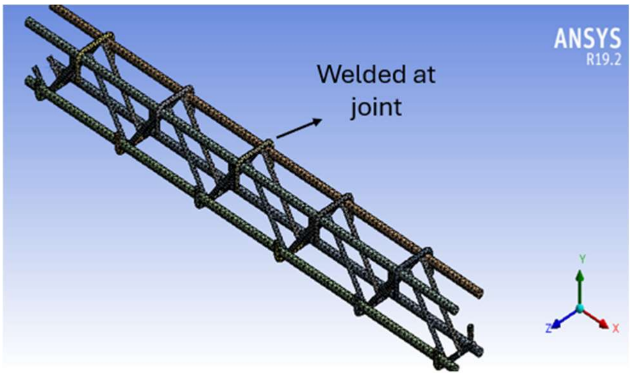

Figure 15. Meshed Model for WWTB Reinforcement (Normal orientation).

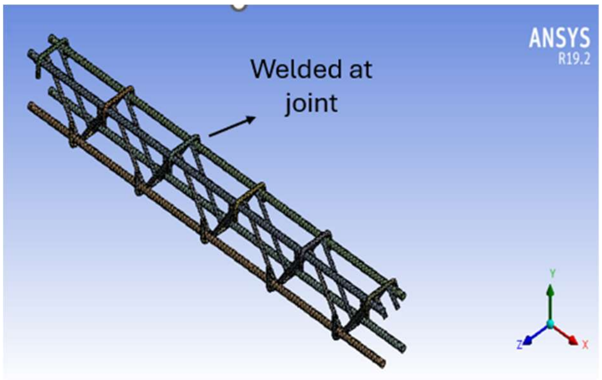

Figure 16. Meshed model for WWTB reinforcement (Flipped orientation).

2.6. Boundary condition and load increment

The beam had fixed support at one end. Typically, plastic hinges in terms of boundary conditions are between 0.1 and 0.2 for a cantilever beam; consideration of 0.2 is more common. Fixed support was selected directly from the ANSYS Workbench command list (**Figure 17**). The total moment applied to the finite-element model is divided into a series of increments called steps. A step corresponds to a set of loads for which you want to obtain a solution and review results. Solving an analysis with nonlinearities requires convergence of an iterative solution procedure. The convergence of this solution procedure requires the load to be applied gradually with solutions carried out at intermediate load values. These intermediate solution points within a step are referred to as sub-steps. Essentially, a sub-step is an increment of load within a step at which a solution is carried out. The moment is applied on the free end as shown in **Figure 18**, and the number of steps and sub-steps is shown in **Figure 19**.

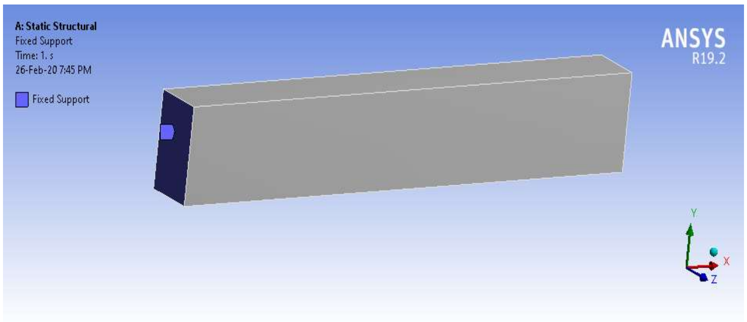

Figure 17. Assigned fixed support.

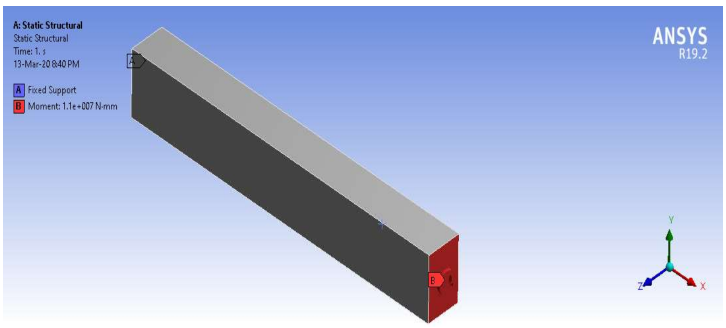

Figure 18. Assigned moment.

Step Controls	
Number Of Steps	1.
Current Step Number	1.
Step End Time	1. s
Auto Time Stepping	On
Define By	Substeps
Initial Substeps	50.
Minimum Substeps	50.
Maximum Substeps	250.

Figure 19. Number of steps and sub-steps.

2.7. Solution and post-processing

The meshed models were analyzed. After the analysis, required data or images are extracted from ANSYS for further analysis. For further analysis, the essential data are loading values, stress distribution, and maximum equivalent stress in both concrete and steel. In addition, all the values were imported from ANSYS to Excel for making the necessary graphs. Moreover, the required screenshots were taken from ANSYS. Thereafter, all the graphs and analysis are presented in the 'Result and Discussion' section.

3. Result and discussion

In an under-reinforced beam, steel yields while concrete remains under-stressed. Cracks appear on the beam as the stress in the steel reaches the yield point. The torsional moment capacity of the beams until the steel yields is presented in **Figures 20** and **21** for *fc'* of 22.92 MPa and 43.47 MPa, respectively. The ultimate torsional moment of each beam is presented in **Table 1**. Note that the FWWTB-type beam was out of experimental data. The other beams show a little variation in results ranging from 3.25%–6.95%. Also, the information related to the ultimate angle of twist is shown in the table. The ultimate torsional moment of each type of beam was taken and compared with NRSB. The comparison is shown in **Figures 22** and **23** for 22.92 MPa and 43.47 MPa, respectively. From **Figures 22** and **23**, it can be said that the torsional moments of +0.5%, −10.1%, and +12.1% are seen for NWWTB, FWWTB, and WRSB with respect to NRSB for the concrete compressive strength of 22.92 MPa. The respective values are +1.9%, −1.8%, and +6.5% for the concrete compressive strength of 43.72 MPa. Therefore, it can be seen that the WRSB beam has the highest ultimate torsional moment carrying capacity and the ultimate angle of twist, while FWWTB has the lowest in both.

The stress distribution across concrete for NRSB, WRSB, NWWTB, and FWWTB is shown in **Figures 24–27**, respectively. By the visual comparison of **Figures 20** and **21**, it is seen that more stress and moments can be shared by the reinforcement of WRSB compared to others. Also, from **Figures 24–27**, it can be seen that the contribution of reinforcement is more obvious in WRSB and NRSB. FWWTB and NWWTB are showing more red sections than others, having less contribution of reinforcement.

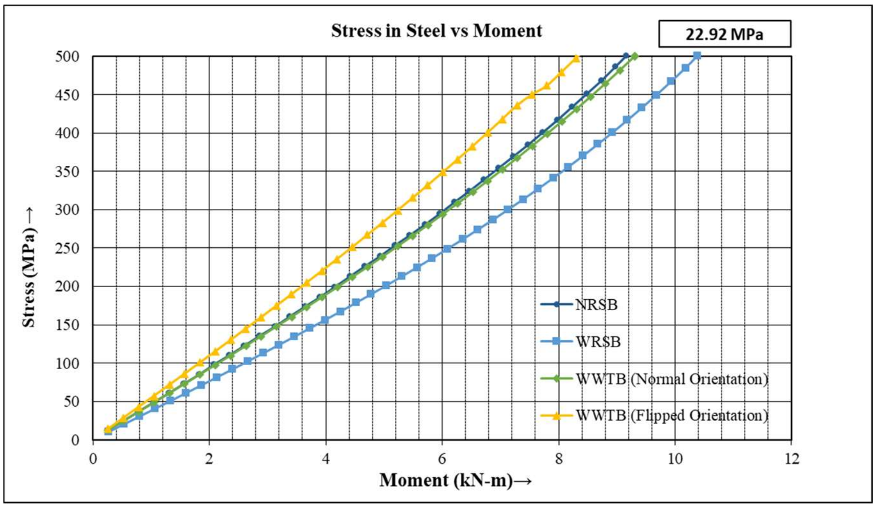

Figure 20. Stress vs applied moment for *fc′* of 22.92 MPa.

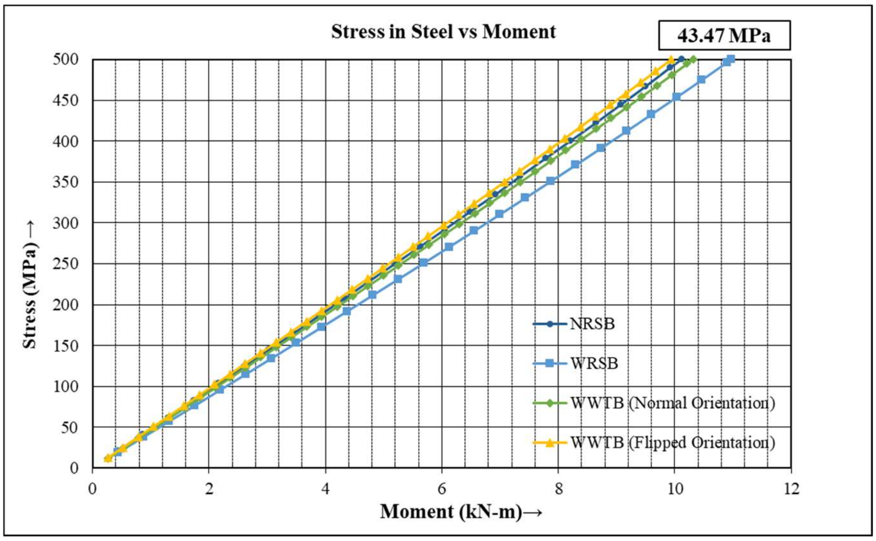

Figure 21. Stress vs applied moment for *fc′* of 43.47 MPa.

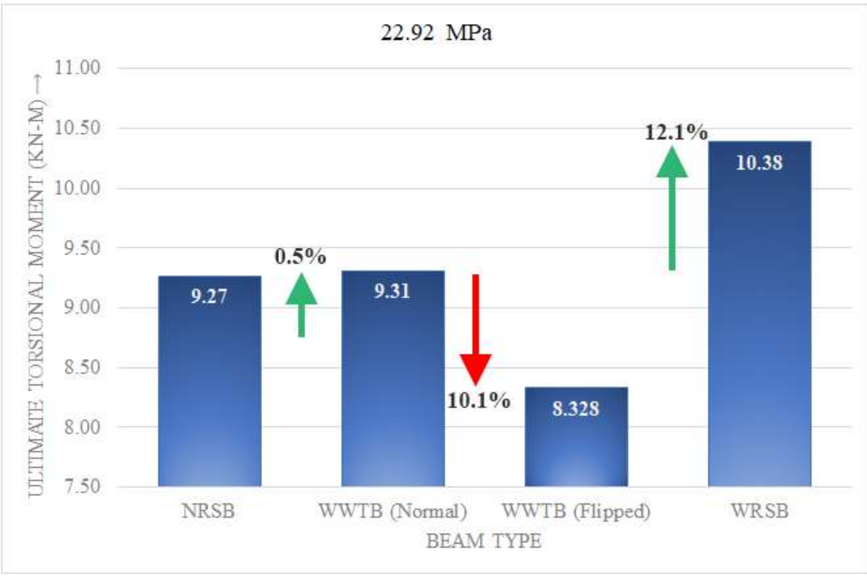

Figure 22. Increment compared to NRSB for *fc′* of 22.92 MPa.

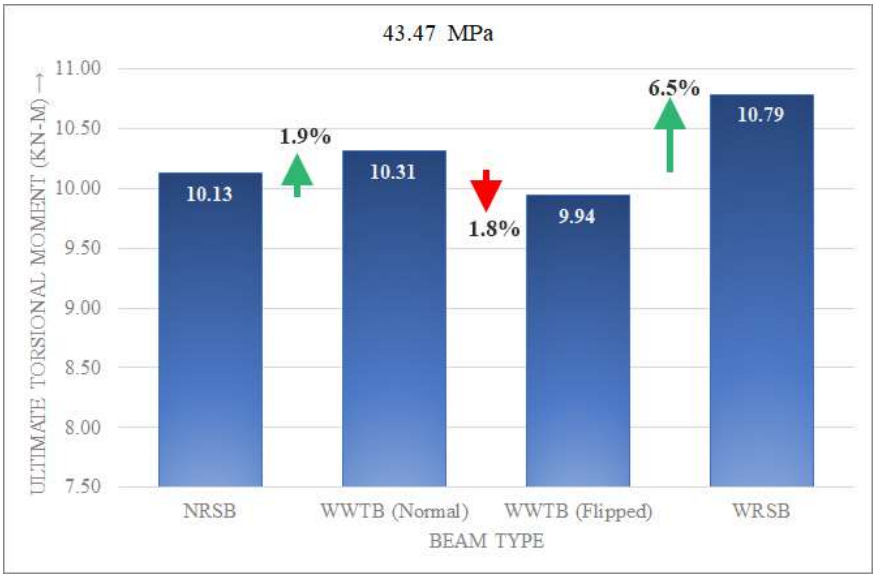

Figure 23. Increment compared to NRSB for *fc'* of 43.47 MPa.

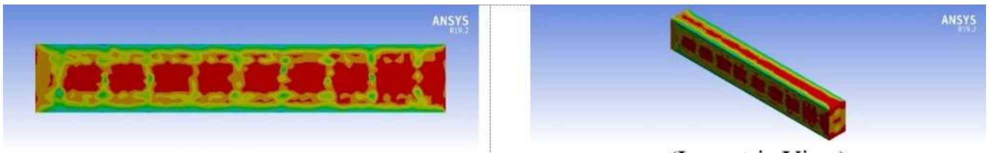

(Side View) (Isometric View)

Figure 24. Stress distribution across NRSB.

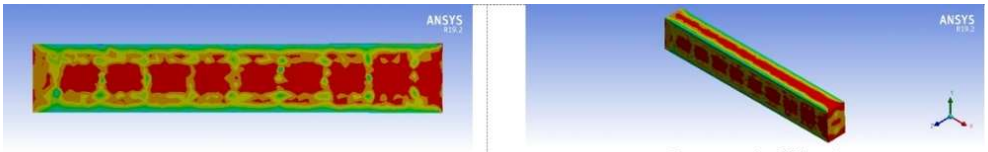

(Side View) (Isometric View)

Figure 25. Stress distribution across WRSB.

(Side View) (Isometric View)

Figure 26. Stress distribution across NWWTB.

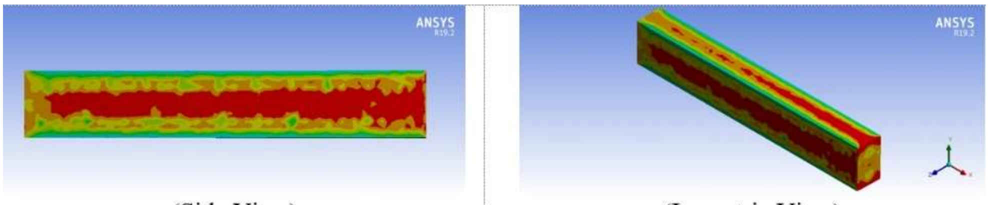

(Side View) (Isometric View)

Figure 27. Stress distribution across FWWTB.

Table 1. Ultimate torsional moment and angle of twist for each *fc'*.

28-day compressive strength of Concrete, *fc'*	Beam Type	FEA Ultimate Torsional Moment	FEA Ultimate Angle of twist, Ø (Rad/m) × 10^{-3}
22.92 MPa	NRSB	9.26	13.00
	WRSB	10.38	14.73
	NWWTB	9.31	13.20
	FWWTB	8.33	11.81
43.72 MPa	NRSB	10.13	10.43
	WRSB	10.78	11.11
	NWWTB	10.31	10.62
	FWWTB	9.94	10.40

4. Conclusion

For reinforced concrete beams, torsional failure is a brittle type failure. The pattern of shear reinforcement plays an important role in preventing this problem. In this research, FE analysis (supported by ANSYS and SOLIDWORKS) is done for varying patterns of shear reinforcement (i.e., Welded Rectangular Stirrup Beam (WRSB), Normal Welded Warren Truss-shaped Beam (NWWTB), and Flipped Welded Warren Truss-shaped Beam (FWWTB), keeping the performance of the conventional one in parallel (i.e., Non-Welded Rectangular Stirrup Beam (NRSB)). In conclusion, the following comments can be presented:

a) For both values of compressive strength, WRSB had the highest ultimate torsional moment and angle of twist capacity.
b) After WRSB, NWWTB, followed by NRSB, showed better performance. FWWTB showed the lowest capacity.
c) For WRSB, torsional moment was 12.1% and 6.5% higher than NRSB for concrete compressive strength of 22.92 MPa and 43.47 MPa, respectively, whereas the torsional moment for NWWTB was 0.5% and 1.9% higher than NRSB for the two values, and FWWTB performed worse than NRSB by 10.1% and 1.8% higher than NRSB for concrete compressive strength of 22.92 MPa and 43.47 MPa, respectively.
d) Experimental investigation ensuring the mentioned physical condition (in Section 3.0 Research Method) can give a better understanding. More analysis can be done using ANSYS Mechanical APDL, particularly using the CPT 215 element, in order to get the cracking pattern and angle of twist from ANSYS Mechanical APDL.
e) The result got from this study may be useful for further study in this field as well as for practicing professionals.
f) The data presented in this paper is entirely generated through software operations, with no validation against experimental data. As a result, there is an opportunity to strengthen the findings through experimental investigation. This limitation should be acknowledged as a potential shortcoming of the current study.

Author contributions: Conceptualization, WJJ, RUA and HMAM; methodology,

HMAM, WJJ and RUA; software, WJJ and RUA; validation, WJJ and RUA; formal analysis, RUA; investigation, RUA; resources, MAI; data curation, WJJ and RUA; writing—original draft preparation, WJJ, RUA and HMAM; writing—review and editing, HMAM and MAI; visualization, HMAM and MAI; supervision, HMAM; project administration, HMAM; funding acquisition, WJJ and RUA. All authors have read and agreed to the published version of the manuscript.

Conflict of interest: The authors declare no conflict of interest.

Abbreviations

E_c	Modulus of elasticity of concrete
f	Stress at any strain, ε, MPa
ε	Strain at stress, f
ε_0	Strain at ultimate compressive strength, f_c'
NRSB	Non-welded Rectangular Stirrup Beam
WRSB	Welded Rectangular Stirrup Beam
NWWTB	Normal Welded Warren Truss-shaped Beam and
FWWTB	Flipped Welded Warren Truss-shaped Beam

References

1. Panchacharam S, Belarbi A. Torsional behavior of reinforced concrete beams strengthened with FRP composites. First FIB Congress, Osaka, Japan. 2002; 1: 01-110.
2. Deifalla A, Ghobarah A. Full torsional behavior of RC beams wrapped with FRP: Analytical model. Journal of Composites for Construction. 2010; 14(3): 289-300.
3. Mahzuz HMA, Ahmed M, Islam MdM, et al. Influence of truss-type and welded reinforcement in concrete beam. International Journal of Structural Engineering. 2022; 12(2): 144. doi: 10.1504/ijstructe.2022.121911
4. Prasanthni P, Priya B, Palanisamy T, et al. Enhancing PVCC beam performance through PVA fiber and basalt fabric in sustainable construction: ductility, strength, and energy absorption improvements. Matéria (Rio de Janeiro). 2024; 29(1). doi: 10.1590/1517-7076-rmat-2023-0299
5. Mohanraj R, Senthilkumar S, Padmapoorani P. Mechanical properties of RC beams with AFRP sheets under a sustained load. Materiali in Tehnologije. 2022; 56(4). doi: 10.17222/mit.2022.481
6. Demir A, Caglar N, Ozturk H, et al. Nonlinear finite element study on the improvement of shear capacity in reinforced concrete T-Section beams by an alternative diagonal shear reinforcement. Engineering Structures. 2016; 120: 158-165. doi: 10.1016/j.engstruct.2016.04.029
7. Saju SM, Usha S. Study on flexural strength of truss reinforced concrete beams. International Research Journal of Engineering and Technology. 2016: 1541-1545.
8. Al-Nasra MM, Asha NM. Shear reinforcements in the reinforced concrete beams. American Journal of Engineering Research (AJER). 2013; 2(10): 191-199.
9. Khan MU, Fahad M, Shahzada K. Shear Capacity Assessment of Reinforced Concrete Beams Using Swimmer Bars as Shear Reinforcement. International Journal of Civil Engineering. 2020; 2(6): 14-20. doi: 10.14445/23488352/ijce-v2i6p104
10. Mahzuz HMA, Nury AH, Ahmed M, et al. Enhancing torsional performance of reinforced concrete beams: a comparative analysis of shear reinforcement strategies. Discover Civil Engineering. 2024; 1(1). doi: 10.1007/s44290-024-00029-3
11. Khan HU. Identification of shear cracks in reinforced beams using finite element method (ANSYS). Pakistan Journal of Science. 2014: 66(1).
12. Subramani T, Manivannan R, Kavitha M. Crack identification in reinforced concrete beams using ANSYS software. J. Eng. Res. Appl. 2014; 4(6): 133-141.
13. Cucchiara C, La Mendola L, Papia M. Effectiveness of stirrups and steel fibres as shear reinforcement. Cement and Concrete

Composites. 2004; 26(7): 777-786. doi: 10.1016/j.cemconcomp.2003.07.001
14. Nilson AH, Dolan CW, Darwin D. Design of concrete structures, 14th ed. McGraw-Hill Education; 2009.
15. Saifullah I, Hossain MA, Uddin SMK, et al. Nonlinear analysis of RC beam for different shear reinforcement patterns by finite element analysis. International Journal of Civil & Environmental Engineering. 2011; 11(1): 63-74.
16. Hasan K, Alam MM, Mahzuz HMA, Hasan K. FE simulation of reinforced concrete beam using ANSYS for several patterns of shear reinforcement. In: Proceedings of the 5th International Conference on Advances in Civil Engineering, CUET, Chattogram-4349; 2021; Bangladesh. pp.143-150.
17. Dahmani L, Khennane A, Kaci S. Crack identification in reinforced concrete beams using ANSYS software. Strength of Materials. 2010; 42(2): 232-240. doi: 10.1007/s11223-010-9212-6
18. Vasudevan G, Kothandaraman S, Azhagarsamy S. Study on Non-Linear Flexural Behavior of Reinforced Concrete Beams Using ANSYS by Discrete Reinforcement Modeling. Strength of Materials. 2013; 45(2): 231-241. doi: 10.1007/s11223-013-9452-3
19. Vasudevan G, Kothandaraman S. Behavior prediction of RC beams-comparison of experimental, FEA and analytical methods. In: IEEE-International Conference on Advances in Engineering, Science and Management (ICAESM-2012). pp. 365-370
20. Kandekar SB, Talikoti RS. Study of torsional behavior of reinforced concrete beams strengthened with aramid fiber strips. International Journal of Advanced Structural Engineering. 2018; 10(4): 465-474. doi: 10.1007/s40091-018-0208-y
21. Rathi S, Kandekar S, Talikoti R. Strengthening of RC beam using carbon and aramid fiber for its torsional behavior. Int J Sci Res Dev. 2015; 3(07): 416-419.
22. Azimi M, Ponraj M, Bagherpourhamedani A, et al. Shear capacity evaluation of reinforced concrete beams: finite element simulation. Jurnal Teknologi. 2015; 77(16). doi: 10.11113/jt.v77.6400
23. Vasudevan G, Kothandaraman S. Parametric study on Nonlinear Finite Element Analysis on flexural behaviour of RC beams using ANSYS. International journal of civil & structural engineering. 2011; 2(1): 98-111.
24. Fanning P. Nonlinear Models of Reinforced and Post-tensioned Concrete Beams. Electronic Journal of Structural Engineering. 2001; 1(2): 111-119. doi: 10.56748/ejse.1182
25. Musmar MA, Rjoub MI, Hadi MA. Nonlinear finite element analysis of shallow reinforced concrete beams using SOLID65 element. Elastic. 2006; 25743: 0-3.
26. Mohanraj R, Vidhya K. Evaluation of compressive strength of Euphorbia tortilis cactus infused M25 concrete by using ABAQUS under static load. Materials Letters. 2024; 356: 135600. doi: 10.1016/j.matlet.2023.135600
27. Krishnasamy R, Johnson SC, Kumar PS, et al. Experimental Investigation of Lateral Load Test on Diagonal Braced 3M Glass Fiber Reinforced Polymer Transmission Tower. Power Research. A Journal of CPRI. 2024: 225-231. doi: 10.33686/pwj.v19i2.1150
28. Ravikumar K, Palanichamy S, Singaram CJ, Rajendran M. Crushing performance of pultruded GFRP angle section with various connections and joints on lattice towers. Matéria (Rio de Janeiro). 2023; 28(1): e20230003
29. Ravikumar K, Singaram CJ, Palanichamy S, et al. Testing and Evaluation of Buckling and Tensile Performance of Glass Fiber–Reinforced Polymer Angle Section with Different Joints/Connections. Journal of Testing and Evaluation. 2024; 52(1): 621-638. doi: 10.1520/jte20230010
30. MacGregor JG, Wight JK, Teng S, Irawan P. Reinforced concrete: Mechanics and design. Prentice Hall Upper Saddle River, NJ; 1997. p. 3.